Biophysical Journal 112 (2017) 288-299

Electrostatic Stabilization plays a Central Role in Autoinhibitory Regulation of the Na^+,K^+-ATPase

Running title: Regulation of the Na^+,K^+-ATPase
Key words: eosin; Gouy-Chapman theory; stopped-flow kinetics; fluorescence; ionic strength; buffer effects

Q. Jiang, A. Garcia, M. Han, F. Cornelius, H.-J. Apell, H. Khandelia, R. J. Clarke

ABSTRACT: The Na^+,K^+-ATPase is present in the plasma membrane of all animal cells. It plays a crucial role in maintaining the Na^+ and K^+ electrochemical potential gradients across the membrane, which are essential in numerous physiological processes, e.g. nerve, muscle and kidney function. Its cellular activity must, therefore, be under tight metabolic control. Consideration of eosin fluorescence and stopped-flow kinetic data indicates that the enzyme's E2 conformation is stabilized by electrostatic interactions, most likely between the N-terminus of the protein's catalytic α-subunit and the adjacent membrane. The electrostatic interactions can be screened by increasing ionic strength, leading to a more evenly balanced equilibrium between the E1 and E2 conformations. This represents an ideal situation for effective regulation of the Na^+,K^+-ATPase's enzymatic activity, since protein modifications which perturb this equilibrium in either direction can then easily lead to activation or inhibition. The effect of ionic strength on the E1:E2 distribution and the enzyme's kinetics can be mathematically described by the Gouy-Chapman theory of the electrical double-layer. Weakening of the electrostatic interactions and a shift towards E1 causes a significant increase in the rate of phosphorylation of the enzyme by ATP. Electrostatic stabilization of the Na^+,K^+-ATPase's E2 conformation, thus, could play an important role in regulating the enzyme's physiological catalytic turnover.

The Na^+,K^+-ATPase is a member of the P-type ATPase family. Other prominent members of this family include the sarcoplasmic reticulum and plasma membrane Ca^{2+}-ATPases and the H^+,K^+-ATPase of the stomach mucosa (1). The Na^+,K^+-ATPase is a transmembrane protein expressed in all animal cells. It utilizes energy from ATP hydrolysis to transport three Na^+ ions out of and two K^+ ions into the cell per ATP molecule hydrolyzed. The electrochemical potential gradients of these ions which the Na^+,K^+-ATPase thus maintains across the cell membrane are essential to fundamental cell functions such as solute transport and cell volume regulation (2). The protein consists of a catalytic α-subunit with a large cytoplasmic domain, a smaller β-subunit with a small extracellular domain and, in various tissues, an even smaller subunit with a single membrane-spanning α helix, in the case of kidney cells the so-called γ-subunit.

Because of Na^+,K^+-ATPase involvement in physiological functions such as nerve, muscle and kidney function, its activity must be under tight metabolic control. Recently it has become clear that many P-type ATPases possess regulatory R domains at either their cytoplasmic N- or C-termini, which have an autoinhibitory effect on pump activity (3-5). In the case of the Na^+,K^+-ATPase it appears that it is the N-terminus which plays a crucial role in controlling the enzyme's conformational transition between the Na^+-stabilized E1 state, which undergoes phosphorylation by ATP, and the K^+-stabilized E2 state, which requires conversion to E1 before ATP phosphorylation can occur (6-8). Removal of the N-terminus either via proteolytic cleavage (7,9) or mutagenesis (8) was found to cause a shift in the protein's conformational equilibrium towards E1. In fact an involvement of the Na^+,K^+-ATPase N-terminus in the E2-E1 transition was already shown by Jørgensen and collaborators (9-12) from proteolytic digestion experiments. In the E1 state trypsin cleaves rapidly at Lys 30 (T_2 site) and subsequently at Arg 262 (T_3 site), whereas in the E2 state it cleaves first at Arg 438 (T_1 site) and afterwards at Lys 30. This suggests that in the E2 state Lys 30 of the α-subunit is initially protected from trypsin attack. Because the N-terminus is highly charged and Jørgensen found that trypsinolysis of the bond 30-31 was strongly dependent on ionic strength (12), he and Collins suggested (9) that a salt bridge of the N-terminus is involved in the E1-E2 transition and that this could be a feature of regulation of mammalian kidney Na^+,K^+-ATPase.

In what might initially seem like unrelated experiments it has been found that the kinetics of Na^+-dependent phosphorylation of mammalian kidney Na^+,K^+-ATPase by ATP are strongly dependent on buffer composition (13,14). Such effects have sometimes been referred to as a Na^+-like buffer effect, stabilizing the E1 conformation (14). However, Lüpfert et al. (13) found that the observed kinetic effects of a range of buffers were only dependent on the degree of ionization of the buffer, not on their chemical structures. This result suggests a non-specific charge-dependent origin, rather than binding to a specific site on the protein. Thus, the shift towards E1 and consequent increase in rate of phosphorylation can more accurately be described as an ionic strength effect, and parallels the behavior observed by Jørgensen (12) via trypsinolysis. At the time, Lüpfert et al. (13) described their experimental kinetic data phenomenologically using a Hill coefficient to account for the dependence of their observed rate constant, k_{obs}, on buffer concentration. In the light of mounting evidence for the involvement of ionic interactions of the N-terminus in regulation of the Na^+,K^+-ATPase, here we reanalyze the data of Lüpfert et al. (13) mechanistically within the framework of an ionic-strength-dependent change in the state of an electrostatic attraction and discuss the relevance of the attraction for Na^+,K^+-ATPase regulation. In kinetic measurements on the E2 → E1 transition in isolation (i.e. uncoupled from ATP phosphorylation), we previously showed (15) from the concentration dependence of the observed rate constants that salt must be acting on

the E2 conformation. The attraction being weakened by ionic strength is, thus, presumably one which initially stabilizes the E2 conformation.

It is important to point out that in spite of the publication of X-ray crystal structures of the Na^+,K^+-ATPase (16-19) and other P-type ATPases (20-22), as pointed out by Morth et al. (4), "no structural information is yet available to describe the molecular mechanism of P-type ATPase autoinhibition". In the case of the Na^+,K^+-ATPase, the major reason for this is that the N-terminus is not resolved in any of the crystal structures, presumably because it is too flexible. This stresses the necessity for mechanistic studies in order to provide an understanding of Na^+,K^+-ATPase regulation.

MATERIALS AND METHODS

Enzyme and reagents

Na^+,K^+-ATPase-containing membrane fragments from the outer medulla of pig kidney were purified as described by Klodos et al. (23). They were stored in a pH 7.4 buffer containing 25 mM imidazole, 250 mM sucrose and 1 mM EDTA. The specific ATPase activity at 37°C and pH 7.4 was measured according to Ottolenghi (24). The activity of the preparation used was 1365 μmol ATP hydrolysed h^{-1} (mg of protein)$^{-1}$ at saturating substrate concentrations and the protein concentration was 6.2 mg mL^{-1}. The protein concentration was determined according to the Peterson modification (25) of the Lowry method (26) using bovine serum albumin as a standard.

The origins of the various reagents used were as follows: EDTA (99%, Sigma, Castle Hill, Australia), Tris(hydroxymethyl)aminomethane (99%, Alfa Aesar, Heysham, UK), imidazole (≥99%, Sigma), eosin Y (C.I. 45380, BDH, Kilsyth, Australia), L-histidine (≥99.5%, Fluka, Castle Hill, Australia), and HCl (0.1 N Titrisol solution, Merck, Kilsyth, Australia).

Eosin fluorescence measurements

All fluorescence measurements were carried out using an RF-5301 PC spectrofluorophotometer (Shimadzu, Kyoto, Japan) with 1 cm pathlength quartz microcuvettes. 1000 μL of pH 7.4 buffer (0.1 mM EDTA and varying concentrations of either Tris or imidazole), 39 μL of Na^+,K^+-ATPase-containing membrane fragments (6.2 mg mL^{-1} in 25 mM imidazole, 250 mM sucrose and 1 mM EDTA, pH 7.4) and 2.9 μL of eosin (11 μM in water) were consecutively added to the cuvette. In the case of the histidine titration, EDTA was omitted because of the poor buffering capacity of histidine at pH 7.4. The final ionic strength of the solution in the cuvette was calculated based on the major contribution from the components of the titration buffer (i.e. Tris, imidazole, or histidine) and a small contribution from the imidazole of the enzyme suspension buffer. Dilution of both the titration buffer and the enzyme suspension buffer was taken into account in the calculation of both the final ionic strength and the buffer concentrations. Fluorescence intensity values for each buffer concentration and excitation wavelength were averaged over five individual measurements. The temperature was maintained at 24ºC via a circulating water bath. The value of λ_{em} was 550 nm (bandwidth 5 nm) with an OG530 cut-off filter (Schott, Mainz, Germany) in front of the photomultiplier. At each of the excitation wavelengths, 490 nm and 535 nm, the apparent background fluorescence was subtracted prior to calculating the fluorescence ratio, $R = F_{490}/F_{535}$. The background level was determined at an excitation wavelength of 400 nm, at which eosin doesn't undergo excitation.

The final Na^+,K^+-ATPase concentration in the cuvette was 230 μg/ml. This concentration was chosen based on previous studies by Skou and Esmann (27,28) in order to saturate the eosin with protein and ensure that all of the measured fluorescence derives from protein-

bound eosin and any fluorescence from eosin in the neighboring aqueous solution can be neglected.

Experimental data analysis and simulation

Nonlinear regression fitting of experimental data was carried out via the commercially available program Origin 8.5.1 (OriginLab, Northampton, MA). Simulations of the effects of fit parameters on the expected experimental outcome were performed using Berkeley-Madonna 8.3.18 (University of California, Berkeley). Alignment of the sequences of the Na^+,K^+-ATPase α_1 subunit were conducted using the BLASTP tool (29) of the National Center for Biotechnology Information, US National Library of Medicine, National Institutes of Health (http://blast.ncbi.nlm.nih.gov/Blast.cgi).

Molecular dynamics simulations

All-atom simulations were performed using GROMACS version 5.1.2 (30-34), with the CHARMM36 force field with CMAP correction (35-38). Water was explicitly incorporated into the simulations by using the TIP3P water model (35) with Lennard-Jones interactions on all hydrogen atoms. A periodic boundary condition was applied. A 12 Å cutoff was used for the non-bonded neighbor list, which was updated every 10 steps. Van der Waals interactions were switched off after 12 Å. Electrostatic interactions were treated with the particle mesh Ewald (PME) method (39,40). All systems were minimized using the steepest descent algorithm, followed by a 50 ns equilibration and a subsequent 500 ns production run. Five copies of each trajectory from different initial states were investigated. During each equilibration run the temperature was kept constant at 303.15 K by using the Berendsen thermostat (41). After equilibration the temperature of the system was maintained at 303.15 K with the Nose-Hoover thermostat (42,43). The pressure was set to a value of 1 bar with semi-isotropic pressure coupling, realized with the Parrinello-Rahman barostat (44) after equilibration with the Berendsen barostat (41). The Linear Constraint Solver (LINCS) algorithm (45) was used to constrain all hydrogen-containing covalent bonds. A 2 fs time step was used and trajectories were sampled every 50 ps. The data analysis was carried out using GROMACS. The snapshots shown in the figures were rendered using Visual Molecular Dynamics (VMD) (46).

The initial N-terminus conformation of the pig kidney Na^+,K^+-ATPase α-subunit was predicted by QUARK, an *ab initio* protein folding and protein structure prediction algorithm (47). The first 28 residues of the protein were modelled using the first 10 residues from the PDB:3B8E (16) crystal structure (residues 19 to 28). CHARMM-GUI (48-52) was used to construct the bilayer membrane system which consist of 1-palmitoyl-2-oleoyl-*sn*-glycero-3-phosphocholine (POPC) and 1-palmitoyl-2-oleoyl-*sn*-glycero-3-phosphoserine (POPS). The membrane was constructed of 108 lipids with the cytoplasmic leaflet containing 20 mol% POPS. POPC has been used earlier as an effective lipid matrix to analyze ion pumps (53,54). POPS was included on the cytoplasmic side of the membrane in order to approximately reproduce the content of negatively charged lipid headgroups which surround the protein in its native membrane (55). To mimic the tethered N-terminus, the last residue, Leu28, was placed at the same position as in the crystal structure using the Orientations of Proteins in Membranes database (56) (28.7 Å above the lipid phosphate groups of the upper leaflet) and restrained with a harmonic force of 1,000 kJ mol^{-1} nm^{-2} during the simulation. The entire system was hydrated by 6,646 water molecules and kept electroneutral by 11 Na^+ counterions.

RESULTS

Effect of ionic strength on the E1-E2 conformational distribution

Before analyzing the effect of ionic strength on the kinetics of phosphorylation of the Na^+,K^+-ATPase by ATP it is necessary to establish the conformation in which the enzyme is starting. To do this we have modified a method developed by Skou and Esmann (27,28) utilizing the fluorescent dye eosin Y (hereafter simply referred to as eosin). From the extensive investigations of Skou, Esmann and Fedosova (27,28,57), it appears to be the case that eosin binds directly to the ATP binding site of the protein's α-subunit. The affinity of this site for ATP changes from a low affinity in the E2 conformation to a high affinity in the E1 conformation, indicating that there must be some conformational reorganization of the ATP binding site associated with the E2-E1 transition. An opening of the cytoplasmic headpiece consisting of the nucleotide binding (N), phosphorylation (P) and actuator (A) domains and changes in their relative positions have in fact been found from X-ray crystal studies to accompany the E2-E1 transition for the sarcoplasmic reticulum Ca^{2+}-ATPase (58,59). As a consequence of these structural rearrangements, eosin dye molecules which are bound to the ATP binding site undergo a shift of their fluorescence excitation spectrum when the Na^+,K^+-ATPase shifts between the E2 and E1 conformations. Using Na^+ to induce the E1 conformation and K^+ to induce the E2 conformation, Skou and Esmann (27) showed that there is a red shift (i.e. a shift to longer wavelengths) when the enzyme converts from E2 to E1. Here we found a similar effect when the ionic strength is increased by increasing the concentration of Tris (see Fig. 1), imidazole or histidine, indicating that high ionic strength favors the E1 conformation over E2.

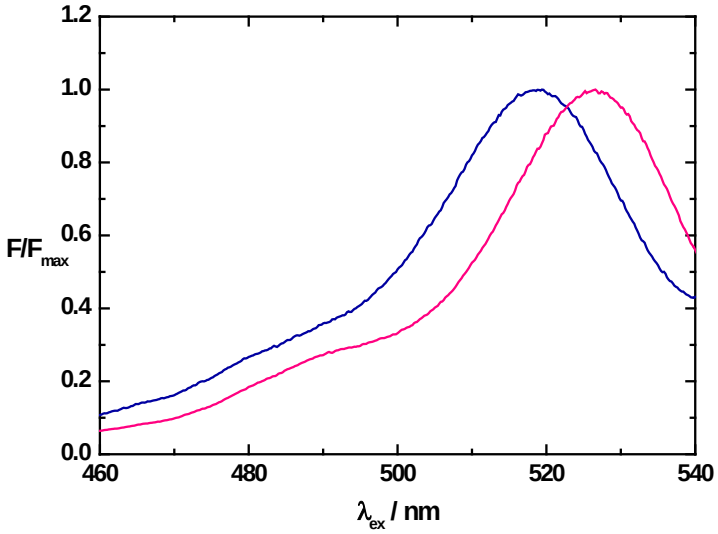

Figure 1: Normalized fluorescence excitation spectra of eosin (29 nM) in the presence of 230 μg/ml of pig kidney Na^+,K^+-ATPase. The blue spectrum is in a solution containing 1 mM Tris (I = 0.86 mM) and the red spectrum is in a solution containing 75 mM Tris (I = 63 mM). Each solution contained 0.1 mM EDTA (pH = 7.4, 24 ºC). The emission wavelength was 550 nm (+OG530 cutoff filter). The bandwidths for both the excitation and emission were 5 nm.

It is worthwhile noting here that the study of ionic strength, I, effects on the Na^+,K^+-ATPase are complicated by the fact that the cations of most salts normally used for the variation of ionic strength (e.g. Na^+, K^+, Rb^+, Cs^+) are either substrates or competitive inhibitors of the Na^+,K^+-ATPase. Interference with the ion transport sites can be minimized by using large organic cations such as Tris, imidazole or histidine. Here we calculate I from the Tris, imidazole or histidine concentration by taking into account their degrees of

ionization of 83.6%, 26.2% and 4.2%, respectively, at pH 7.4, calculated from their pKa values of 8.11 for Tris, 6.95 for imidazole and 6.04 for histidine (60) using the Henderson-Hasselbalch equation. To quantify the shift in the eosin fluorescence excitation spectrum we have devised a ratiometric method, whereby the fluorescence excitation ratio, *R*, is defined as the ratio of the fluorescence emitted at 550 nm using either 490 nm or 535 nm as the excitation wavelength, i.e. $R = F_{490}/F_{535}$. The two wavelengths were chosen because one is on the blue side of the dye's excitation maximum and one is on the red side, and this then gives a wide variation in the value of *R* as the protein moves between the E2 and E1 conformations. The ratiometric method has the advantage over the method used by Skou and Esmann (27,28) and other researchers (57,61,62), who quantified the enzyme's conformational shift between E1 and E2 by measuring fluorescence intensity at a single wavelength, in that the ratiometric method is insensitive to small variations in the dye's concentration. It is, therefore, a useful method for equilibrium fluorescence titrations, such as those reported here, in which rapid data acquisition isn't necessary.

The effect of Tris, imidazole and histidine concentration on the fluorescence ratio, *R*, of eosin bound to pig kidney Na^+,K^+-ATPase is shown in Fig. 2. In each case there is a drop in the value of *R* with increasing concentration. The effectiveness of the buffers in causing the drop increases in the order Tris > imidazole > histidine. Control experiments showed that in buffer solution in the absence of protein *R* was independent of the buffer concentration and had a value of 0.81 (± 0.02). Thus, the decrease in *R* in the presence of the Na^+,K^+-ATPase can confidently be attributed to the effect of the buffers on protein conformation. A decrease in *R* corresponds to a red shift of the fluorescence excitation spectrum and a shift in the protein's conformational equilibrium from E2 to E1, as described earlier.

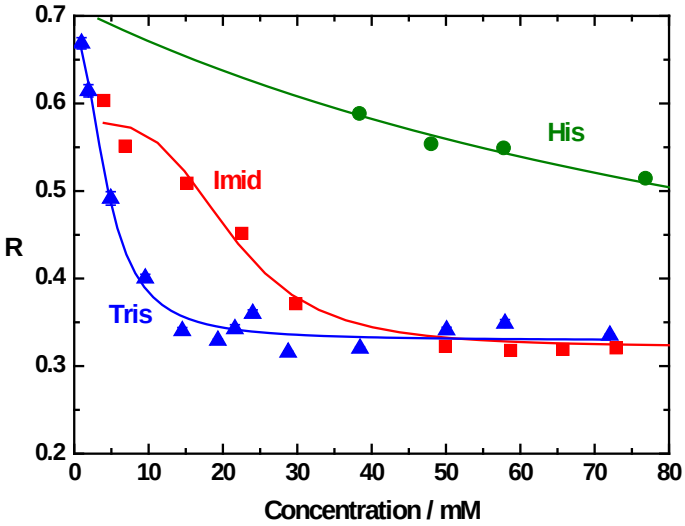

Figure 2: Effect of concentration of the buffers Tris, imidazole and histidine on the fluorescence ratio, *R*, of eosin noncovalently bound to pig kidney Na^+,K^+-ATPase. *R* is defined as the fluorescence intensity ratio using excitation wavelengths of 490 nm and 535 nm, i.e., $R = F_{490}/F_{535}$, at an emission wavelength of 550 nm. A decrease in *R* corresponds to a decrease in the proportion of the enzyme in the E2 conformation and hence an increase in the proportion in the E1 conformation. All other experimental conditions were as described in Fig. 1. The solid lines represent non-linear least squares fits to the experimental data using the Hill equation (Tris and imidazole) or a hyperbolic saturation curve (histidine). The $K_{0.5}$ values determined were 4.5 (± 0.5) mM, 21 (± 1) mM, and 126 (± 70) mM for Tris, imidazole and histidine, respectively. In the case of histidine, measurements were performed up to 190

mM, but only the lowest concentrations are shown on the graph for comparison with the other two buffers. Experiments at histidine concentrations above 200 mM were not possible because of the buffer's solubility limit.

That the effect of the buffers on the E2-E1 transition is not due to their uncharged forms is evidenced by the fact that 3-5 fold higher concentrations of imidazole and 20-30 fold higher concentrations of histidine are required to observe a similar effect to Tris. This can be explained by the different degrees of ionization of the buffers at pH 7.4. The degree of ionization of Tris is 3.2 times higher than that of imidazole and 20.0 times higher than that of histidine. These factors are also reflected in their half-saturating concentrations, $K_{0.5}$, which were determined from fits of the experimentally determined R values to either the phenomenological Hill equation or a hyperbolic saturation curve (see Fig. 2). The values of $K_{0.5}$ obtained were 4.5 (± 0.5) mM for Tris, 21 (± 1) mM for imidazole and 126 (± 70) mM for histidine. The $K_{0.5}$ value for imidazole is a factor of 4.7 (± 0.6) higher than that of Tris, and the $K_{0.5}$ value for histidine is a factor of 28 (± 16) higher than that of Tris. Bearing in mind that no corrections for non-ideal behavior have been taken into consideration, these factors are comparable to the factors one would expect based on the degrees of ionization of the buffers if the enzyme had no preference for $TrisH^+$ over $imidazoleH^+$ or $histidineH^+$. This is in spite of their very different chemical structures (Tris is an aliphatic compound whereas imidazole is aromatic and histidine is an amino acid).

Thus, it seems unlikely that the buffer cations are causing the shift to the E1 conformation by binding preferentially to a specific binding site on the protein when it is in the E1 conformation. This would, furthermore, be incompatible with the results of the kinetic experiments of Humphrey et al. (15), which indicated that the salt-induced shift towards the E1 conformation is due to an interaction with enzyme in the E2 conformation, not E1. The results are, however, consistent with an ionic strength-mediated effect, which is, therefore, how the data has been treated here. Our attribution of the buffer-induced shift towards the E1 conformation to an ionic strength effect rather than to specific binding is also consistent with recent NMR results of Middleton et al. (63), who found different chemical shifts of ATP caused by binding to the nucleotide binding site depending on whether the formation of the E1 conformation was promoted by the addition of Na^+ or $TrisH^+$ ions. From their results Middleton et al. (63) were able to conclude, in agreement with earlier suggestions (64), that $TrisH^+$ does not bind to the Na^+,K^+-ATPase ion transport sites.

The effect of I on the fluorescence ratio, R, of eosin bound to pig kidney Na^+,K^+-ATPase is shown in Fig. 3. The experimental results shown in Fig. 3 were obtained using Tris, imidazole or histidine to vary I. From a comparison of the results shown in Figs. 2 and 3, it can be seen that, although the buffers cause very different concentration dependencies of R, once the concentrations are converted into ionic strength the results from all three buffers are superimposable. This is further evidence that the effect being observed is arising from the ionic strength of the solution, not from binding to a specific site within the protein. The ionic strength dependence of the conformation equilibrium, and therefore of R can be quantitatively explained by the Gouy-Chapman theory of the electrical double layer (65,66), as described in the following section.

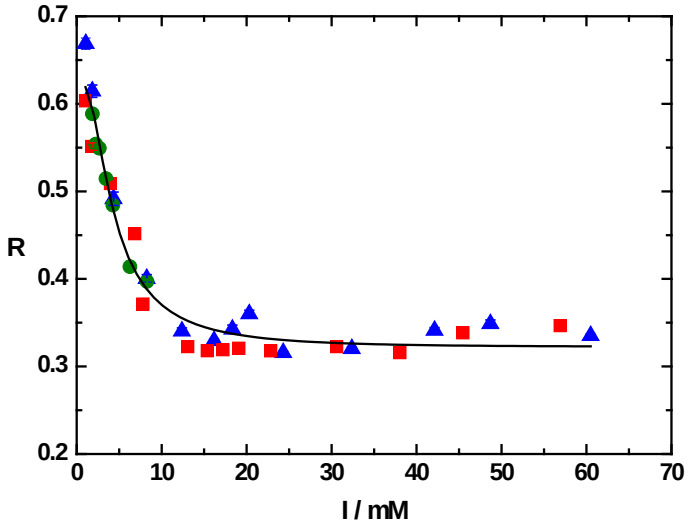

Figure 3: Effect of ionic strength, *I*, on the fluorescence ratio, *R*, of eosin noncovalently bound to pig kidney Na^+,K^+-ATPase. *R* is defined as the fluorescence intensity ratio using excitation wavelengths of 490 nm and 535 nm, i.e., $R = F_{490}/F_{535}$, at an emission wavelength of 550 nm. A decrease in *R* corresponds to a decrease in the proportion of the enzyme in the E2 conformation and hence an increase in the proportion in the E1 conformation. *I* was controlled by the concentration of the buffer. The points were obtained using the buffers Tris (blue triangles), imidazole (red squares) and histidine (green circles). All other experimental conditions were as described in Fig. 1. The solid line represents a non-linear least squares fit of Eqs. 2, 3, 6 and 10 to the experimental data. The values of the parameters derived from the fit were: R_1 = 0.02 (± 0.03), R_2 = 0.62 (± 0.02), σ = 0.023 (± 0.009) Cm^{-2} and *r* = 7 (± 2) nm. The value of R_1 is indistinguishable from zero, which implies that if the enzyme shifted totally into the E1 conformation, the eosin spectrum would shift so far to the red that zero fluorescence intensity would be measured at 490 nm. The value of σ corresponds to a value of 0.014 (± 0.006) e_0nm^{-2}.

Application of the Gouy-Chapman theory to the E1-E2 transition of the Na^+,K^+-ATPase

According to the Gouy-Chapman theory, as long as the surface potential is not too large, i.e. ≤ 25 mV, the electrical potential, ψ, in the solution adjacent to a charged surface can be considered to decay exponentially as the distance, *r*, from the surface increases. Thus,

$$\psi = \psi_0 \exp\left(-r / l_D\right) \qquad (1)$$

where ψ_0 is the electrical potential at the surface and l_D is the Debye length, which is defined by the following expressions:

$$l_D = \frac{1}{F}\sqrt{\frac{\varepsilon_0 \varepsilon RT}{2I}} \qquad (2), \qquad I = \frac{1}{2}\sum_{i=1}^{n} c_i z_i^2 \qquad (3)$$

F is here Faraday's constant, ε_0 is the electrical permittivity of a vacuum, ε is the dielectric constant of the medium surrounding the particle (80 for an aqueous solution), *R* is the ideal gas constant, *T* is the absolute temperature and *I* is the ionic strength of the solution. c_i and z_i

are the concentrations and valences of each type ion in solution, respectively. Making use of Gauss's law together with Eq. 1 it can be shown that the surface potential, ψ_0, is given by:

$$\psi_0 = \frac{\sigma l_D}{\varepsilon_0 \varepsilon} \qquad (4)$$

σ is here the surface charge density of the particle. Substituting for ψ_0 from Eq. 4 into Eq. 1 then yields:

$$\psi = \frac{\sigma l_D}{\varepsilon_0 \varepsilon} \exp\left(-r / l_D\right) \qquad (5)$$

Now, the energy of interaction between a charge on a protein molecule and another charged surface is given by the product of the charge and the electrical potential difference between the charge and the surface. There may be many discrete charge-charge interactions. However, for simplicity and to demonstrate the principle of the effect of ionic strength on the conformational state of the protein, here we consider a macroscopic overall (molar) energy of interaction, ΔE, which is given by:

$$\Delta E = -\frac{F \sigma l_D}{\varepsilon_0 \varepsilon} \exp\left(-r / l_D\right) \qquad (6)$$

The negative value of ΔE in Eq. 6 implies an attractive electrostatic interaction, e.g. such as a salt bridge, as proposed by Jørgensen and Collins (9). If the electrostatic interactions were repulsive, e.g. between protein segments of like charge, then the negative sign would have to be removed.

Let us assume now that an equilibrium exists between protein molecules with either intact (E2) or broken (E1) electrostatic interactions with an equilibrium constant K:

Broken $\overset{K}{\rightleftharpoons}$ Intact

If one assumes that the strength of electrostatic forces, described by Eq. 6, are the dominant factor in determining whether the electrostatic interactions are broken or intact, ΔE can be taken as an approximation of the standard Gibbs free energy change associated with this equilibrium. In this case ΔE is related to the equilibrium constant K by:

$$K = \exp\left(-\Delta E / RT\right) \qquad (7)$$

Now, if one defines the degree of transition between the intact (i) and broken states (b) as x, this is related to K and ΔE by:

$$x = \frac{c_i}{c_b + c_i} = \frac{K}{K+1} = \frac{\exp\left(-\Delta E / RT\right)}{\exp\left(-\Delta E / RT\right)+1} \qquad (8)$$

Similarly, the degree to which the interaction is broken is given by:

$$1 - x = \frac{1}{1+\exp\left(-\Delta E / RT\right)} \qquad (9)$$

Thus, Eqs. 2, 6 and 9 allow one to simulate the expected dependence of the state of the protein's electrostatic interaction and the E1-E2 distribution on the ionic strength, *I*, of the surrounding solution, provided that the surface charge density, σ, and the distance, *r*, over which the electrostatic interaction occurs can be estimated.

If the conformational transition between E1 and E2 is determined by the strength of the protein's electrostatic interaction, as the results in Fig. 2 would indicate, then it follows that *x* (see Eq. 8) corresponds to the fraction of enzyme in the E2 conformation and 1 – *x* (see Eq. 9) corresponds to the fraction of enzyme in the E1 conformational state. The dependence of the eosin fluorescence ratio, *R*, on *I* is then given by:

$$R = R_2 + \frac{(R_1 - R_2)}{1 + \exp\left(-\Delta E / RT\right)} \qquad (10)$$

R_2 is here the limiting value of *R* when the enzyme is fully in the E2 conformational state at low ionic strength with electrostatic interactions at their strongest. Similarly, R_1 is the corresponding limiting value of *R* when the enzyme is fully in the E1 conformational state at high ionic strength when electrostatic interactions have been fully screened.

Since phosphorylation of the Na^+,K^+-ATPase by ATP only occurs from the E1 conformation, it follows that the rate of phosphorylation of the Na^+,K^+-ATPase by ATP should also be modulated by the protein's electrostatic interaction. Thus, the observed rate constant, k_{obs}, for phosphorylation will also depend on whether the interaction is intact or broken and should follow the same dependence on *I* as for *R* (see Eq. 10). Hence, an analogous expression can be written for k_{obs}:

$$k_{obs} = k_2 + \frac{(k_1 - k_2)}{1 + \exp\left(-\Delta E / RT\right)} \qquad (11)$$

k_2 is here the limiting value of k_{obs} for phosphorylation when the enzyme is fully in the E2 conformational state at low ionic strength with electrostatic interactions at their strongest prior to mixing with ATP. Similarly, k_1 is the corresponding limiting value of k_{obs} at high ionic strength when the enzyme is fully in the E1 conformational state prior to mixing with ATP and when electrostatic interactions have been fully screened.

Effect of ionic strength on the kinetics of Na^+,K^+-ATPase phosphorylation by ATP

Figs. 4A and 4B show the stopped-flow kinetic data of Lüpfert et al. (13), obtained using rabbit and pig kidney Na^+,K^+-ATPase, respectively. The kinetics of Na^+-dependent phosphorylation of the enzyme by ATP were measured by incubating the enzyme initially in buffer of varying concentrations of Tris and then simultaneously mixing rapidly with ATP, NaCl and $MgCl_2$. Rather than plot the measured k_{obs} values as a function of the Tris concentration used, as Lüpfert et al. (13) did, in Fig. 4 we have replotted k_{obs} against the ionic strength, *I*, by taking into account the percentage of Tris ionization, as described above for the eosin measurements. It is evident that the kinetics are significantly accelerated on increasing *I*. The increase in k_{obs} can now be interpreted as being due to the weakening of electrostatic interactions, allowing the enzyme to convert from the E2 conformation into the E1 conformation. The lower k_{obs} value found when the enzyme is present in a low ionic strength solution can be explained by the slow rate-determining conversion of the enzyme from the E2 into the E1 conformation prior to phosphorylation of the protein. Slow phosphorylation of enzyme in the E2 conformation can be excluded as an explanation for the

observed data, because this would lead to biphasic kinetic behavior in the stopped-flow experiments, with the amplitudes of the two phases varying with *I*. Such behavior was not observed. Weakening of the electrostatic interaction of the E2 conformation appears to be necessary to allow ATP phosphorylation of the enzyme.

Fits of the newly derived theory expressed in Eq. 10 to the stopped-flow kinetic data of Lüpfert et al. (13) are shown in Figs. 4A and 4B. Eqs. 2, 3 and 6 were used simultaneously to calculate ΔE and derive the expected dependence of k_{obs} on *I*. For rabbit kidney Na^+,K^+-ATPase the values of the parameters derived from the fit are: k_2 = 88 (± 6) s^{-1}, k_1 = 325 (± 35) s^{-1}, σ = 0.016 (± 0.008) Cm^{-2} and r = 2.2 (± 1.9) nm. For pig kidney Na^+,K^+-ATPase the corresponding values are: k_2 = 61 (± 4) s^{-1}, k_1 = 242 (± 11) s^{-1}, σ = 3 (± 7) Cm^{-2} and r = 13 (± 5) nm. The charge density values correspond to 0.10 (± 0.05) e_0nm^{-2} and 21 (± 45) e_0nm^{-2} for the rabbit and pig enzymes, respectively, which, taking into account the large errors of the values, are not significantly different. Although it is difficult to derive accurate values for the parameters σ and r because they are coupled in determining ΔE (Eq. 6), the results show that the model described above, whereby the strengths of electrostatic interactions of the protein are predicted via the Gouy-Chapman theory, adequately reproduces the observed experimental behavior. No specific buffer-induced change in protein conformational state need be assumed.

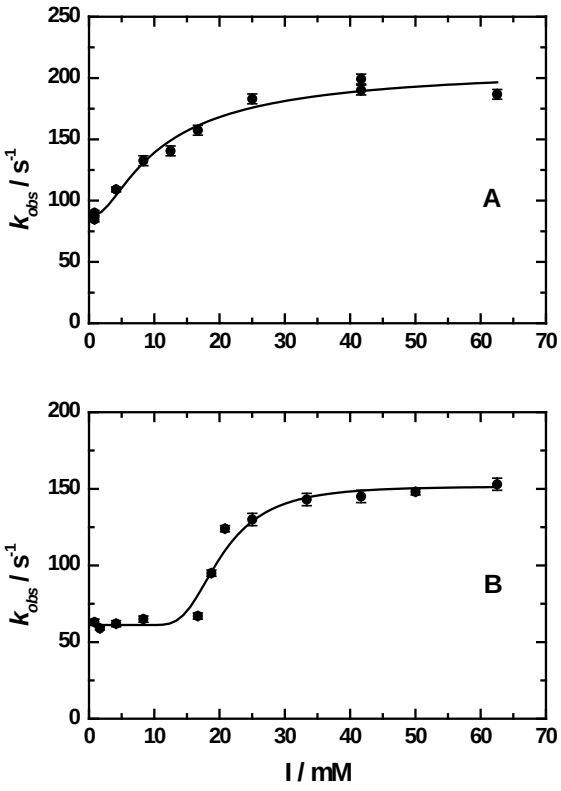

Figure 4: Effect of ionic strength, *I*, of the preincubation buffer solution on the observed rate constant, k_{obs}, for phosphorylation of rabbit kidney (A) and pig kidney (B) Na^+,K^+-ATPase by ATP (pH 7.4, 24ºC).
The ionic strength of the solution was controlled by varying the Tris concentration (from 1 – 75 mM). In addition to Tris, the preincubation buffer contained 0.1 mM EDTA. Phosphorylation was induced by mixing with an equal volume of phosphorylation-initiating solution (30 mM Imidazole, 5 mM $MgCl_2$, 1 mM EDTA, 130 mM NaCl and 2 mM Tris/ATP, pH 7.4, 24ºC). The kinetics were measured via stopped-flow fluorimetry using the voltage-

sensitive fluorescent membrane probe RH421 as described by Lüpfert *et al*. (13). The protein concentration prior to mixing was 20 μg/ml.
The solid lines represent non-linear least squares fits of Eqs. 2, 3, 6 and 11 to the experimental data.

The experimental results show that for pig kidney Na^+,K^+-ATPase the dependence of k_{obs} on I is sigmoidal, whereas for rabbit kidney Na^+,K^+-ATPase the sigmoidicity is smaller and the curve almost looks hyperbolic. Theoretical simulations based on Eqs. 2, 3, 6 and 11 indicate that the major determining factor in the degree of sigmoidicity is the surface charge density, σ. Thus, a higher value of σ leads to stronger electrostatic interactions and a greater sigmoidicity. The amino acid sequences of the rabbit and pig enzymes are almost identical (97% identity and 99% homology for the entire α-subunit based on a BLASTP alignment (27)). Therefore, one would not expect large differences in behavior of the two enzymes if the electrostatic interactions were within the protein's polypeptide chain or between polypeptide chains on adjacent molecules within the membrane. A more likely cause would be interactions between charges on the protein and its adjacent membrane. The membrane lipid composition of the pig and rabbit plasma membranes would be expected to be quite different, in part because of different diets of the two animals, i.e. rabbits are herbivores and pigs are omnivores.

A final important point to note is that the saturating value of k_{obs} at high I is not equal to k_1. Even though the electrostatic interactions are completely abolished at high I, the saturating value of k_{obs} is much lower than k_1, both for the rabbit and pig enzymes. From Eq. 10, setting ΔE to 0, the saturating value of k_{obs} is given by $(k_2 + k_1)/2$, i.e. the average between the limiting values of the rate constants at zero and high ionic strength. This average value equals 206 s^{-1} for rabbit enzyme and 151 s^{-1} for pig. The reason for this is that at $\Delta E = 0$ there is no net electrostatic driving force modulating the distribution of the enzyme between E1 and E2, and hence, based on electrostatics alone, the E1 and E2 states are equally likely. Therefore, at high I the E1 and E2 conformational states would be expected to be in a dynamic equilibrium. If the degree of conversion of the enzyme towards E1 or towards E2 could be further changed via repulsion or attraction, respectively, there is large scope for either increasing the rate of phosphorylation further or decreasing the rate again. This could potentially have great significance for regulation of the Na^+,K^+-ATPase *in vivo*, as will be described in the Discussion.

Molecular Dynamics Simulations of the N-terminus

Published pig kidney Na^+, K^+-ATPase crystal structures in the E2 (PDB 3B8E) and the E1 state (PDB 3WGU and 4HQJ) are lacking structural information on the N-terminus of the α-subunit of the protein. In the E2 structure (3B8E) the first 18 amino acids could not be resolved (16). In the case of the E1 structures, the first 22 amino acids are missing in the 3WGU structure (18) and the first 31 amino acids are missing in the 4HQJ structure (19). The situation is very similar for the published E2 structure of shark rectal gland Na^+,K^+-ATPase (2ZXE), where the first 26 amino acids could not be resolved (17). As explained in the Introduction, because this portion of the protein is intimately involved in the E1-E2 conformational transition, we decided to carry out a computational prediction of its conformation and investigate its potential for interaction with the membrane surface, as suggested by the equilibrium fluorescence titrations and the kinetic measurements described in the previous sections.

All-atom molecular dynamics (MD) simulations of the N-terminus of the pig kidney Na^+,K^+-ATPase α-subunit with the transmembrane portions of the protein embedded within a

model POPC-POPS membrane were conducted as described under Materials and Methods. The structure of the entire protein with the predicted N-terminus structure added to the E2 crystal structure (PDB 3B8E) is shown in Fig. 5a. A closeup of the interaction of the N-terminus with the membrane is shown in Fig. 5b. Among the lysine residues of the N-terminus, Lys16, Lys17, and Lys20 are closest to the membrane surface (see Fig. 5b) and show a high radial distribution function (g(r)) peak with the POPS headgroup (see Fig. 5c). Interestingly, this group of lysine residues is located at the end of the helix (residue number from 16 to 21), which is in close contact with the membrane surface. As indicated by the density profiles of the N-terminus and the phosphate groups of the lipid headgroups, the N-terminus of the protein remains bound to the membrane, surface driven by electrostatic interactions with the negatively charged membrane (see Fig. 6). This is consistent with an interaction between the N-terminus and the membrane as the source of the experimentally observed effect of ionic strength on the E1-E2 distribution described earlier.

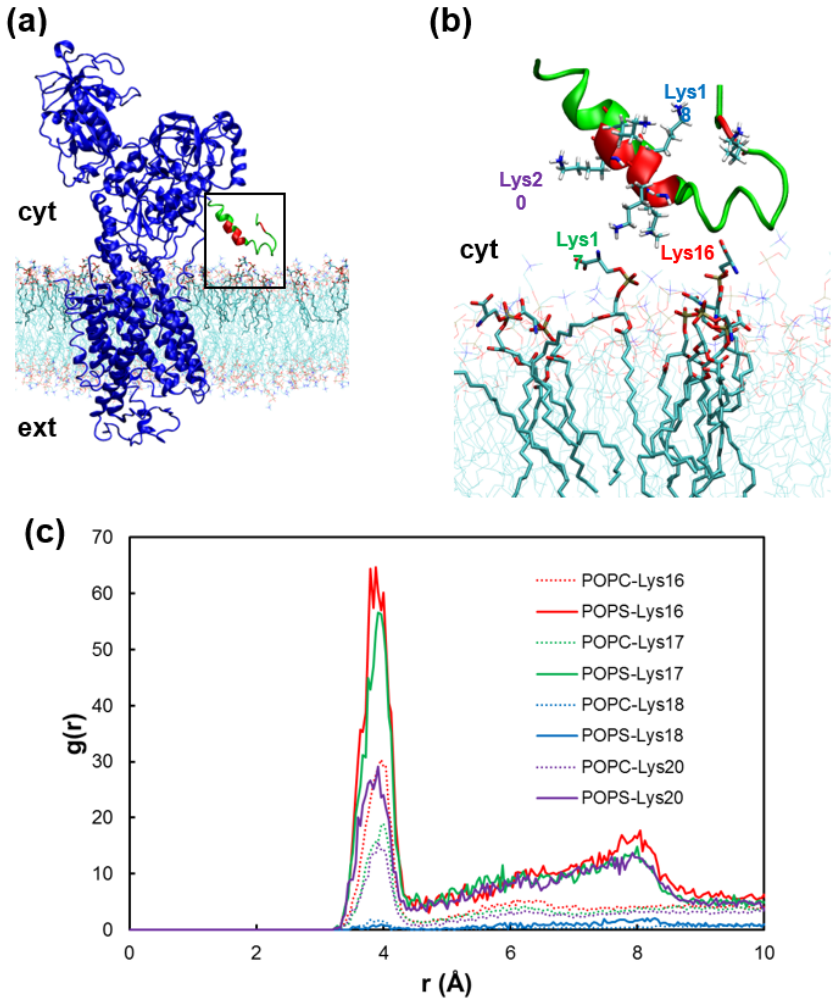

Figure 5: (a) Na^+, K^+-ATPase embedded in a POPC (line)/POPS (liquorice) lipid bilayer. For clarity water molecules are not shown. The Na^+, K^+-ATPase is shown in blue. The N-terminus is shown in green, except for its lysine residues, which are shown in red. Only the N-terminus was simulated with MD. (b) Close-up of the N-terminus in the black square of (a). The snapshot is picked from the 500 ns MD trajectory. (c) Radial distribution function between the nitrogen atoms in the side chains of Lys16, Lys17, Lys18 and Lys20 and phosphorus atom in POPS and POPC.

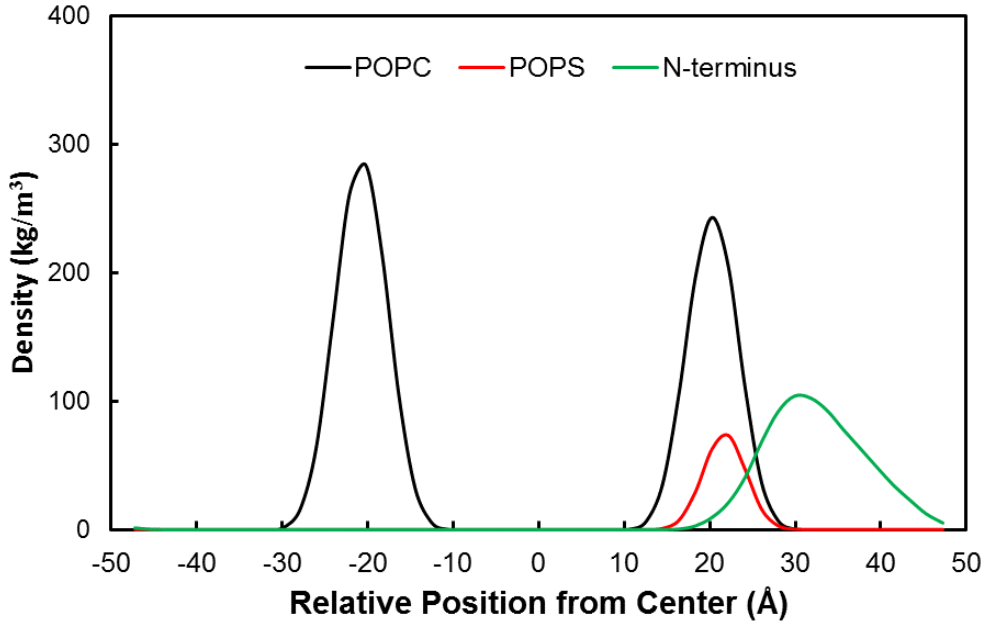

Figure 6: Density profile of the phosphate group of the POPC/POPS membrane and the N-terminus, with respect to the bilayer center. Data are sampled from a 500 ns MD trajectory**.**

DISCUSSION

The analysis of the ionic strength dependence of the kinetics of Na^+,K^+-ATPase phosphorylation by ATP carried out here has shown that the observed experimental kinetic behavior is consistent with an ionic-strength-induced change in the protein's conformational state due to screening of protein surface charge. To be more precise, a breaking of electrostatic attractions in the E2 conformation leads to a promoted transition of the enzyme into the E1 conformation with a resultant increase in the rate of phosphorylation. After electrostatic interactions have been completely screened by ionic strength, van der Waals forces would still be present and these are likely to prevent a complete shift into the E1 state.

We consider that the most likely site of the electrostatic interactions responsible for the E1-E2 conformational shift is between the cytoplasmic N-terminus of the Na^+,K^+-ATPase's α-subunit and the adjacent membrane. The reasons for this statement are presented below. As pointed out by Jørgensen and Collins (9), the N-terminus is highly charged. Within the first 50 amino acid residues the pig kidney Na^+,K^+-ATPase contains 10 positively charged lysine residues, 3 positively charged arginine residues, 7 negatively charged aspartic acid residues and 6 glutamic acid residues. For the rabbit enzyme the numbers of each of the charged amino acids along the same sequence are the same except for one additional lysine residue. Thus, although highly charged, the N-terminus is roughly net neutral. Furthermore, as pointed out in the Introduction, there is a large body of research data indicating movement of the N-terminus associated with the E1-E2 transition and its effect on the position of the E1-E2 conformational equilibrium (6-12). In addition, Liu et al. (67) found that cleavage of the protein at its N-terminus by chymotrypsin significantly increases the protein's phosphorylation capacity. From mutagenesis studies, Scanzano et al. (8) even localized the groups of amino acids within the N-terminus of the rat α_1 subunit of the Na^+,K^+-ATPase which play the most dominant roles in modulating the E1-E2 conformational transition, i.e. 31KKE and 47HRK, which both form part of small putative α-helical segments. The first

coincides very well with the T_2 trypsin cleavage site identified by Jørgensen and collaborators (9-12), which is known to move during the E1-E2 transition.

Because the ionic strength dependence of the ATP phosphorylation kinetics of Na^+,K^+-ATPase from pig and rabbit kidney (see Fig. 4) appears quite different in spite of very similar amino acid sequences (97% identity and 99% homology for the entire α-subunit) of the two enzymes, it seems most likely that the electrostatic interactions are not between the N-terminus and other charged residues on the protein. In contrast to the similar protein structures, the plasma membrane compositions of pigs and rabbits are known to be very different (68), and, even between preparations of the Na^+,K^+-ATPase-containing membrane fragments used in the studies described here, there is likely to be some variation in membrane composition. Thus, it seems more probable that the electrostatic interactions are between the N-terminus and charges on the headgroups of lipids in the adjacent membrane. This suggestion is further supported by recent results of Zhou et al. (5) which provided direct evidence for an autoinhibitory interaction between the C-terminus of a different P-type ATPase, a yeast phospholipid flippase, and phosphatidylinositol 4-phosphate (PI(4)P) in the membrane.

It appears likely that an interaction of the N-terminus with anionic lipids in the membrane surrounding the protein would be facilitated by the large number of lysine residues the N-terminus possesses. It is well documented, in particular from research into the membrane-binding activity of antimicrobial peptides, that the basic positively charged amino acid residues lysine and arginine promote membrane binding (69-71). An interaction of the N-terminus with FXYD proteins has, however, been suggested (7) as a possible explanation for different effects of N-terminus truncation on the kinetics of shark and pig Na^+,K^+-ATPase. Although this is definitely a possibility, inspection of amino acid sequences of vertebrate gastric H^+,K^+-ATPase shows though that this closely related enzyme also possesses a lysine-rich N-terminus. There appears to be no evidence that the gastric H^+,K^+-ATPase is associated with an FXYD protein. Thus, regardless of whether an FXYD protein is present or not, in our opinion a membrane interaction of the N-terminus seems most likely to be the prime origin of the electrostatic interaction controlling the Na^+,K^+-ATPase E1-E2 distribution.

Analysis of the phospholipid headgroups of the lipids present in rabbit kidney Na^+,K^+-ATPase-containing membrane fragments has shown (55) that they do in fact contain significant amounts of the anionic lipids phosphatidylserine and phosphatidylinositol, i.e., 13.1 and 5.6 mol% of total phospholipid, respectively. Furthermore, it was found (55) that, after SDS treatment of the initial microsomal preparation to obtain purified Na^+,K^+-ATPase, the phosphatidylserine content increased to a level over 60% higher than that of the initial microsomal level, suggesting a preferential association of phosphatidylserine with the Na^+,K^+-ATPase. Lipid analysis is, thus, consistent with the suggestion that the electrostatic interaction being affected by ionic strength is between the N-terminus and anionic lipids surrounding the protein, in particular phosphatidylserine. Based the lipid analysis of 18.7% total anionic lipid (55), one also estimate the surface charge density this would produce. According to X-ray crystallographic measurements of dioleoylphosphatidylcholine on the fully hydrated state (72) the packing density is 1.220 nm^{-2}. Assuming similar packing for phosphatidylserine and phosphatidylinositol, the total density of negative charges from these two lipids would be expected to be around 0.23 $e_0 nm^{-2}$. To within an order of magnitude this value is consistent with the values obtained here from fitting of equilibrium eosin titrations and kinetic data to the Gouy-Chapman-based theory. In the future, when more structural information is available, it is possible that an improved description of the interaction could be achieved by taking into account discrete charge-charge interactions via molecular dynamics simulations.

The effect of ionic strength described here is not the only effect of ionic strength on the Na^+,K^+-ATPase. Fodor et al. (73) found that the addition of salt to an ionic strength of 1 mM protected both shark rectal gland and pig kidney Na^+,K^+-ATPase from thermal denaturation. However, this effect occurs at an ionic strength level ten times lower than the effects discussed here. Rather than being due to intermolecular interactions, the effects seen by Fodor et al. (73) are most likely due to ions binding within individual Na^+,K^+-ATPase molecules and reducing electrostatic repulsions between like-charged amino acid residue side chains.

Now it is important to consider the broader physiological relevance of the results reported here. Under physiological conditions of non-saturating cytoplasmic Na^+ concentrations (in part because of competition from cytoplasmic K^+ ions, which favor the E2 conformation) it is known that the enzyme's phosphorylation by ATP is a major rate-determining step of the pump cycle (74). Therefore, any change in the rate of this reaction step will significantly alter the enzyme's turnover. It is, thus, a key reaction in Na^+,K^+-ATPase regulation. Taken as a whole, the results shown here indicate that under physiological conditions the rate of ATP phosphorylation would be far below its maximum, not just because the cytoplasmic Na^+ concentration is non-saturating, but also because the E1-E2 conformational equilibrium does not fully lie on the side of E1. A far higher rate of phosphorylation could be reached if the protein's conformational equilibrium could be shifted entirely to the E1 side. Therefore, the balanced distribution of the Na^+,K^+-ATPase between the E1 and E2 conformations which is achieved by weakening of salt bridge interactions at physiological ionic strength levels represents an ideal situation for effective regulation of the protein's activity. Any modification to the protein, e.g. phosphorylation by protein kinases (75), which might affect the strength of intermolecular forces between the N-terminus and the membrane surface, would be expected to shift the E1-E2 equilibrium, causing a change in the rate of Na^+,K^+-ATPase phosphorylation by ATP and a consequent change in the protein's overall steady-state activity. In fact it has already been shown (76,77), at least in the case of the rat α_1 subunit, that the N-terminus is a target of protein kinase C (PKC), which phosphorylates Ser 18 of the peptide chain. Although this particular amino acid residue is substituted by a glycine in rabbit (also in human) and is missing in pig, the N-terminus of pig, rabbit and human possess three other conserved serine residues which could potentially act as PKC targets (78). Finally, apart from the Na^+,K^+-ATPase, dynamic changes in the E1-E2 conformational equilibrium could also potentially be a molecular mechanism underlying regulation of other P-type ATPases, including the sarcoplasmic reticulum Ca^{2+}-ATPase, responsible for muscle relaxation, and the gastric H^+,K^+-ATPase, which provides the acidic environment necessary for digestion.

AUTHOR CONTRIBUTIONS

Q. J. conducted eosin experiments and assisted in data analysis; A. G. conducted eosin experiments; M. H. carried out molecular dynamics simulations; F. C. purified pig enzyme and suggested the use of eosin; H.-J. A. purified rabbit enzyme; H. K. designed and supervised the molecular dynamics simulations; R. J. C. developed theory, analyzed data, conducted eosin experiments and wrote paper.

ACKNOWLEDGEMENT

The authors thank Prof. Promod Pratap, University of North Carolina Greensboro, and Dr. Ilya Reviakine, Karlsruhe Institute of Technology, for helpful discussions. R. J. C. acknowledges with gratitude financial support from the Australian Research Council

(Discovery Grants DP-121003548 and DP-150101112). Molecular dynamics simulations were carried out on the Danish e-Infrastructure Cooperation (DeiC) National HPC Center, ABACUS 2.0 and Horseshoe9 at the University of Southern Denmark. M. H. acknowledges financial support from a Novo Nordisk Foundation Postdoctoral Grant. H. K. is supported by the Lundbeckfonden.

REFERENCES

1. Møller, J. V., B. Juul, and M. le Maire. 1996. Structural organization, ion transport, and energy transduction of P-type ATPases. Biochim. Biophys. Acta – Rev. Biomembr. 1286:1-51.
2. Kaplan, J. H. 2002. Biochemistry of Na,K-ATPase. Annu. Rev. Biochem. 71:511-535.
3. Ekberg, K., M. G. Palmgren, B. Veierskov, and M. J. Buch-Pedersen. 2010. A novel mechanism of P-type ATPase autoinhibition involving both termini of the protein. J. Biol. Chem. 285:7344-7350.
4. Morth, J. P., B. P. Pedersen, M. J. Buch-Pedersen, J. P. Andersen, B. Vilsen, M. G. Palmgren, and P. Nissen. 2011. A structural overview of the plasma membrane Na^+,K^+-ATPase and H^+-ATPase ion pumps. Nat. Rev. Mol. Cell Biol. 12:60-70.
5. Zhou, X., T. T. Sebastian, and T. R. Graham. 2013. Auto-inhibition of Drs2p, a yeast phospholipid flippase, by its carboxyl-terminal. J. Biol. Chem. 288:31807-31815.
6. Wu, C. H., L. A. Vasilets, K. Takeda, M. Kawamura, and W. Schwarz. 2003. Functional role of the N-terminus of Na^+,K^+-ATPase α-subunit as an inactivation gate of palytoxin-induced pump channel. Biochim. Biophys. Acta – Biomembr. 1609:55-62.
7. Cornelius, F., Y. A. Mahmmoud, L. Meischke, and G. Cramb. 2005. Functional significance of the shark Na,K-ATPase N-terminal domain. Is the structurally variable N-terminus involved in tissue-specific regulation by FXYD proteins? Biochemistry 44:13051-13062.
8. Scanzano R., L. Segall, and R. Blostein. 2007. Specific sites in the cytoplasmic N terminus modulate conformational transitions of the Na,K-ATPase. J. Biol. Chem. 282:33691-33697.
9. Jørgensen, P. L., and J. H. Collins. 1986. Tryptic and chymotryptic cleavage sites in sequence of α-subunit of (Na^+ + K^+)-ATPase from outer medulla of mammalian kidney. Biochim. Biophys. Acta 860:570-576.
10. Jørgensen, P. L., E. Skriver, H. Hebert, and A. B. Maunsbach. 1982. Structure of the Na,K-pump: Crystallization of pure membrane-bound Na,K-ATPase and identification of functional domains of the α-subunit. Ann. N. Y. Acad. Sci. 402:207-225.
11. Jørgensen, P. L., and J. P. Andersen. 1988. Structural basis for E1-E2 conformational transitions in Na,K-pump and Ca-pump proteins. J. Membr. Biol. 103:95-120.
12. Jørgensen, P. L. 1975. Purification and characterization of (Na^+,K^+)-ATPase. 5. Conformational-changes in enzyme-transitions between Na-form and K-form studied with tryptic digestion as a tool. Biochim. Biophys. Acta 401:399-415.
13. Lüpfert C., E. Grell, V. Pintschovius, H.-J. Apell, F. Cornelius, and R. J. Clarke. 2001. Rate limitation of the Na^+,K^+-ATPase pump cycle. Biophys. J. 81:2069-2081.
14. Schuurmans Stekhoven, F. M. A. H., H. G. P. Swarts, J. J. H. H. M. De Pont, and S. L. Bonting (1985) Na^+-like effect of imidazole on the phosphorylation of (Na^+ + K^+)-ATPase. Biochim. Biophys. Acta – Biomembr. 815:16-24.
15. Humphrey P., C. Lüpfert, H.-J. Apell, F. Cornelius, and R. J. Clarke (2002) Mechanism of the rate-determining step of the Na^+,K^+-ATPase pump cycle. Biochemistry 41:9496-9507.
16. Morth, J. P., B. P. Pedersen, M. S. Toustrup-Jensen, T. L. Sørensen, J. Petersen, J. P. Andersen, B. Vilsen, and P. Nissen. 2007. Crystal structure of the sodium-potassium pump. Nature 450:1043-1049.
17. Shinoda, T., H. Ogawa, F. Cornelius, and C. Toyoshima. 2009. Crystal structure of the sodium-potassium pump at 2.4 Å resolution. Nature 459:446-450.
18. Kanai, R., H. Ogawa, B. Vilsen, F. Cornelius, and C. Toyoshima. 2013. Crystal structure of a Na^+-bound Na^+,K^+-ATPase preceding the E1P state. Nature 502:201-206.

19. Nyblom, M., H. Poulsen, P. Gourdon, L. Reinhard, M. Andersson, E. Lindahl, N. Fedosova, and P. Nissen. 2013. Crystal structure of Na^+,K^+-ATPase in the Na^+-bound state. Science 342:123-127.
20. Toyoshima, C., M. Nakasako, H. Nomura, and H. Ogawa. 2000. Crystal structure of the calcium pump of sarcoplasmic reticulum at 2.6 Å resolution. Nature 405:647-655.
21. Pedersen, B. P., M. J. Buch-Pedersen, J. P. Morth, M. G. Palmgren, and P. Nissen. 2007. Crystal structure of the plasma membrane proton pump. Nature 450:1111-1114.
22. Wang, K., O. Sitsel, G. Meloni, H. E. Autzen, M. Andersson, T. Klymchuk, A. M. Nielsen, D. C. Rees, P. Nissen, and P. Gourdon. 2014. Structure and mechanism of Zn^{2+}-transporting P-type ATPases. Nature 514:518-522.
23. Klodos, I., M. Esmann, and R. L. Post. 2002. Large-scale preparation of sodium-potassium ATPase from kidney outer medulla. Kidney Int. 62:2097-2100.
24. Ottolenghi, P. 1975. The reversible delipidation of a solubilized sodium-plus-potassium ion-dependent adenosine triphosphatase from the salt gland of the spiny dogfish. Biochem. J. 151:61-66.
25. Peterson, G. L. 1977. A simplification of the protein assay method of Lowry et al. which is more generally applicable. Anal. Biochem. 83:346-356.
26. Lowry, O. H., N. J. Rosebrough, A. L. Farr, and R. J. Randall. 1951. Protein measurement with the Folin phenol reagent. J. Biol. Chem. 193:265-275.
27. Skou, J. C., and M. Esmann. 1981. Eosin, a fluorescent probe of ATP binding to the (Na^+ + K^+)-ATPase. Biochim. Biophys. Acta 6472:232-240.
28. Skou, J. C., and M. Esmann. 1983. The effects of Na^+ and K^+ on the conformational transition of (Na^+ + K^+)-ATPase. Biochim. Biophys. Acta 746:101-113.
29. Altschul, S. F., T. L. Madden, A. A. Schaffer, J. H. Zhang, Z. Zhang, W. Miller, and D. J. Lipman. 1997. Gapped BLAST and PSI-BLAST: a new generation of protein database search programs. Nucleic Acids Res. 25:3389-3402.
30. Berendsen, H. J. C., D. van der Spoel, and R. van Drunen. 1995. GROMACS: A message-passing parallel molecular dynamics implementation. Comput. Phys. Commun. 91:43-56.
31. Van der Spoel, D., E. Lindahl, B. Hess, G. Groenhof, A. E. Mark, and H. J. C. Berendsen. 2005. GROMACS: Fast, flexible, and free. J. Comput. Chem. 26:1701-1718.
32. Hess, B., C. Kutzner, D. van der Spoel, and E. Lindahl. 2008. GROMACS4: Algorithms for highly efficient, load-balanced, and scalable molecular simulation. J. Chem. Theory Comput. 4:435-447.
33. Pronk, S., S. Pall, R. Schulz, P. Larsson, P. Bjelkmar, R. Apostolov, M. R. Shirts, J. C. Smith, P. M. Casson, D. van der Spoel, B. Hess and E. Lindahl. 2013. A high-throughput and highly parallel open source molecular simulation toolkit. Bioinformatics 29:845-854.
34. Abraham, M. J., T. Murtola, R. Schulz, S. Páll, JC Smith, B. Hess, and E. Lindahl. 2015. High performance molecular simulations through multi-level parallelism from laptops to supercomputers. SoftwareX 1-2:19-25.
35. MacKerell, A. D., D. Bashford, M. Bellott, R. L. Dunbrack, J. D. Evanseck, M. J. Field, S. Fischer, J. Gao, H. Guo, S. Ha, D. Joseph-McCarthy, L. Kuchnir, K. Kuczera, F. T. K. Lau, C. Mattos, S. Michnick, T. Ngo, D. T. Nguyen, B. Prodhom, W. E. Reiher, B. Roux, M. Schlenkrich, J. C. Smith, R. Stote, J. Straub, M. Watanabe, J. Wiorkiewicz-Kuczera, D. Yin, and M. Karplus. 1998. All-atom empirical potential for molecular modeling and dynamics studies of proteins. J. Phys. Chem. B 102:3586-3616.
36. MacKerell, A. D., M. Feig, and C. L. Brooks. 2004. Extending the treatment of backbone energetics in protein force fields: Limitations of gas-phase quantum

mechanics in reproducing protein conformational distributions in molecular dynamics simulation. J. Comput. Chem. 25:1400-1415.
37. Bjelkmar, P., P. Larsson, M. A. Cuendet, B. Hess, and E. Lindahl. 2010. Implementation of the CHARMM force field in GROMACS: Analysis of protein stability effects from correction maps, virtual interaction sites, and water models. J. Chem. Theory Comput. 6:459-466.
38. Klauda, J. B., R. M. Venable, J. A. Freitas, J. W. O'Connor, D. J. Tobias, C. Mondragon-Ramirez, I. Vorobyov, A. D. MacKerell, and R. W. Pastor. 2010. Update of the CHARMM all-atom additive force field for lipids: Validation on six lipid types. J. Phys. Chem. B 114:7830-7843.
39. Darden, T. D. York, and L. Pedersen. 1993. Particle mesh Ewald: An $N\cdot\log(N)$ method for Ewald sums in large systems. J. Chem. Phys. 98: 10089-10092.
40. Essmann, U., L. Perera, M. L. Berkowitz, T. Darden, H. Lee, and L. G. Pedersen. 1995. A smooth particle mesh Ewald method. J. Chem. Phys. 103:8577-8593.
41. Berendsen, H. J. C., J. P. M. Postma, W. F. van Gunsteren, A. DiNola, and J. R. Haak. 1984. Molecular dynamics with coupling to an external bath. J. Chem. Phys. 81:3684-3690.
42. Nosé, S. 1984. A unified formulation of the constant temperature molecular dynamics methods. J. Chem. Phys. 81:511-519.
43. Hoover, W. G. 1985. Canonical dynamics: Equilibrium phase-space distributions. Phys. Rev. A 31:1695-1697.
44. Parrinello, M., and A. Rahman. 1981. Polymorphic transitions in single crystals: A new molecular dynamics method. J. Appl. Phys. 52:7182-7190.
45. Hess, B., H. Bekker, H. J. C. Berendsen, and J. G. E. M. Fraaije. 1997. LINCS: A linear constraint solver for molecular simulations. J. Comput. Chem. 18:1463-1472.
46. Humphrey, W., A. Dalke, and K. Schulten. 1996. VMD: Visual molecular graphics. J. Mol. Graph. 14:33-38.
47. Xu, D., and Y. Zhang. 2012. Ab initio protein structure assembly using continuous structure fragments and optimized knowledge-based force field. Proteins 80:1715-1735.
48. Jo, S., T. Kim, V. G. Iyer, and W. Im. 2008. CHARMM-GUI: A web-based graphical user interface for CHARMM. J. Comput. Chem. 29:1859-1865.
49. Brooks, B. R., C. L. Brooks, A. D. MacKerell, L. Nilsson L., R. J. Petrella, B. Roux, Y. Won, G. Archidontis, C. Bartels, S. Boresch, A. Caflisch, L. Caves, Q. Cui, A. R. Dinner, M. Feig, S. Fischer, J. Gao, M. Hodoscek, W. Im, K. Kuczera, T. Lazaridis, J. Ma, V. Ovchinnikov, E. Paci, R. W. Pastor, C. B. Post, J. Z. Pu, M. Schaefer, B. Tidor, R. M. Venable, H. L. Woodcock, X. Wu, W. Yang, D. M. York, and M. Karplus. 2009. CHARMM: The biomolecular simulation program. J. Comput. Chem. 30:1545-1614.
50. Jo, S., J. B. Lim, J. B. Klauda, and W. Im. 2009. CHARMM-GUI membrane builder for mixed bilayers and its application to yeast membranes. Biophys. J. 97:50-58.
51. Lee, J., X. Cheng, J. M. Swails, M. S. Yeom, P. K. Eastman, J. A. Lemkul, S. Wei, J. Buckner, J. C. Jeong, Y. F. Qi, S. Jo, V. S. Pande, D. A. Case, C. L. Brooks, A. D. MacKerell, J. B. Klauda, and W. Im. 2016. CHARMM-GUI input generator for NAMD, GROMACS, AMBER, OpenMM, and CHARMM/OpenMM simulations using the CHARMM36 additive force field. J. Chem. Theory Comput. 12:405-413.
52. Wu, E. L., X. Cheng, S. Jo, H. Rui, K. C. Song, E. M. Davila-Contreras, Y. F. Qi, J. M. Lee, V. Monje-Galvan, R. M. Venable, J. B. Klauda, and W. Im. 2014. CHARMM-GUI membrane builder toward realistic biological membrane simulations. J. Comput. Chem. 35:1997-2004.

53. Musgaard, M., L. Thøgersen, and B. Schiøtt. 2011. Protonation states of important acidic residues in the central Ca^{2+} binding sites of the Ca^{2+}-ATPase: A molecular modeling study. Biochemistry 50:11109-11120.
54. Sonntag, Y., M. Musgaard, C. Olesen, B. Schiøtt, J. V. Møller, P. Nissen, and L. Thøgersen. 2011. Mutual adaptation of a membrane protein and its lipid bilayer during conformational changes. Nature Commun. 2:304.
55. De Pont, J. J. H. H. M., A. Van Prooijen-Van Eeden, and S. L. Bonting. 1978. Role of negatively charged phospholipids in highly purified (Na^+ + K^+)-ATPase from rabbit kidney outer medulla. Studies on (Na^+ + K^+)-activated ATPase, XXXIX. Biochim. Biophys. Acta 508:464-477.
56. Lomize, M. A., A. L. Lomize, I. D. Pogozheva, and H. I. Mosberg. 2006. OPM: Orientations of proteins in membranes database. Bioinformatics 22:623-625.
57. Esmann, M., and N. U. Fedosova. 1997. Eosin as a probe for conformational transitions and nucleotide binding in Na,K-ATPase. Ann. N. Y. Acad. Sci. 834:310-321.
58. Møller, J. V., C. Olesen, A.-M. L. Winther, and P. Nissen. 2010. The sarcoplasmic reticulum Ca^{2+}-ATPase: design of a perfect chemi-osmotic pump. Q. Rev. Biophys. 43:501-566.
59. Toyoshima, C., and F. Cornelius. 2013. New crystal structures of PII-type ATPases: excitement continues. Curr. Opin. Struct. Biol. 23:507-514.
60. Dawson, R. M. C., D. C. Elliott, W. H. Elliott, and K. M. Jones. 1986. Data for Biochemical Research, 3rd ed. Oxford University Press, Oxford, UK. 423-425.
61. Montes, M. R., R. M. González-Lebrero, P. J. Garrahan, and R. C. Rossi. 2004. Quantitative analysis of the interaction between the fluorescent probe eosin and the Na^+/K^+-ATPase studied through Rb^+ occlusion. Biochemistry 43:2062-2069.
62. Montes, M. R., R. M. González-Lebrero, P. J. Garrahan, and R. C. Rossi. 2006. Eosin fluorescence changes during Rb^+ occlusion in the Na^+/K^+-ATPase. Biochemistry 45:13093-13100.
63. Middleton, D. A., N. U. Fedosova, and M. Esmann. 2015. Long-range effects of Na^+ binding in Na,K-ATPase reported by ATP. Biochemistry 54:7041-7047.
64. Fedosova, N. U., and M. Esmann. 2004. Nucleotide binding kinetics of Na,K-ATPase: cation dependence. Biochemistry 43:4212-4218.
65. Adam, G., P. Läuger, and G. Stark. 1988. Physikalische Chemie und Biophysik, 2nd ed. Springer, Berlin, Germany. 276-277.
66. Hiemenz, P. C. 1986. Principles of Colloid and Surface Chemistry, 2nd ed. Marcel Dekker, New York. 686-703.
67. Liu, G., Z. Xie, N. N. Modyanov, and A. Askari. 1996. Restoration of phosphorylation capacity to the dormant half of the α-subunits of Na^+,K^+-ATPase. FEBS Lett. 390:323-326.
68. Yorek, M. A. 1993. Biological distribution. *In* Phospholipids Handbook, G. Cevc, editor. Dekker, New York. 745-775.
69. Zasloff, M. 2002. Antimicrobial peptides of multicellular organisms. Nature 415:389-395.
70. Li, L. B., Vorobyov, I., and T. W. Allen. 2013. The different interactions of lysine and arginine side chains with lipid membranes. J. Phys. Chem B 117:11906-11920.
71. Hädicke, A., and A. Blume. 2016. Binding of the cationic peptide $(KL)_4K$ to lipid monolayers at the air-water interface: Effect of lipid headgroup charge, acyl chain length and acyl chain saturation. J. Phys. Chem. B 120:3880-3887.
72. Lis, L. J., M. McAlister, N. Fuller, R. P. Rand, and V. A. Parsegian. 1982. Interactions between neutral phospholipid-bilayer membranes. Biophys. J. 37:657-666.

73. Fodor, E., N. U. Fedosova, C. Ferencz, D. Marsh, T. Pali, and M. Esmann. 2007. Stabilization of Na,K-ATPase by ionic interactions. Biochim. Biophys. Acta – Biomembr. 1778:835-843.
74. Clarke, R. J., M. Catauro, H. H. Rasmussen, and H.-J. Apell. 2013. Quantitative calculation of the role of Na^+,K^+-ATPase in thermogenesis. Biochim Biophys Acta – Bioenerg. 1827:1205-1212.
75. Mahmmoud, Y. A., and F. Cornelius F. 2002. Protein kinase C phosphorylation of purified Na,K-ATPase: C-terminal phosphorylation sites as the α- and γ-subunits close to the inner face of the plasma membrane. Biophys. J. 82:1907-1919.
76. Chibalin, A. V., C. H. Pedemonte, A. I. Katz, E. Feraille, P. O. Bergren, and A. M. Bertorello. 1998. Phosphorylation of the catalytic α-subunit constitutes a triggering signal for Na^+,K^+-ATPase endocytosis. J. Biol. Chem. 273:8814-8819.
77. Chibalin, A. V., G. Ogimoto, C. H. Pedemonte, T. A. Pressley, A. I. Katz, E. Feraille, P. O. Bergren, and A. M. Bertorello. 1999. Dopamine-induced endocytosis of Na^+,K^+-ATPase is initiated by phosphorylation of Ser-18 in the rat α subunit and is responsible for decreased activity in epithelial cells. J. Biol. Chem. 274:1920-1927.
78. Feschenko, M. S., and K. J. Sweadner. 1995. Structural basis for species-specific differences in the phosphorylation of Na,K-ATPase by protein kinase C. J. Biol. Chem. 270:14072-14077.